Relativistic calculations of $4f$ excitation energies in the rare-earth metals: Further results

J. F. Herbst* and R. E. Watson

Brookhaven National Laboratory, Upton, New York 11973

J. W. Wilkins

Laboratory of Atomic and Solid State Physics, Materials Science Center, Cornell University, Ithaca, New York 14853
(Received 9 December 1977)

We report additional results of our relativistic calculations of $4f$ excitation energies in the rare-earth metals: (i) $4f$ binding energies computed for the atomic configurations used as inputs to our band calculations, as well as for the atomic ground states; (ii) band parameters and $4f$ level positions calculated via the renormalized-atom method, with emphasis on the unoccupied $4f$ levels; (iii) values for U, the Coulomb interaction energy between two $4f$ electrons at the same metallic site; and (iv) simple estimates of cohesive energies. Comparisons are made with experimental values. In particular, we find that our approach works well for estimating U in metals and insulators. The Appendix contains a discussion of the connection between our calculated parameters and those of the Anderson model (as applied to fluctuating valence systems), including dynamic screening effects.

I. INTRODUCTION

Relativistic calculations of occupied $4f$ level positions in the rare-earth metals were described in a previous paper[1] (hereafter referred to as I). The primary purpose of the effort, as well as that of earlier nonrelativistic work,[2] was the development of a viable well-defined technique for theoretically estimating the $4f$ binding energies measured by photoemission experiments. The computations were carried out within the framework of the renormalized-atom procedure, embodying relativistic-Hartree-Fock (RHF) free-atom solutions and the imposition of specific self-consistency criteria in band-potential construction. Total energy differences were used to estimate the $4f$ level energy relative to the Fermi level ϵ_F, a quantity we denote by $\Delta_-(f^n \to f^{n-1})$,

$$\Delta_-(f^n \to f^{n-1}) = E_{\text{metal}}[4f^{n-1}(5d6s)^{m'}]$$
$$- E_{\text{metal}}[4f^n(5d6s)^m].\qquad(1)$$

E_{metal} represents the total energy per unit cell of the metal, m is the valence, or the number of $5d$-$6s$ conduction electrons. We insist upon charge neutrality of the metallic cell excited by photoejection of a $4f$ electron: $m' = m + 1$ in Eq. (1); the agreement of our Δ_- values with experiment suggests that the $4f$ photoemission event corresponds closely to this "complete-screening" limit. In this work we present additional results, among which are estimates of unoccupied $4f$ level energies relative to ϵ_F, $\Delta_+(f^n \to f^{n+1})$,

$$\Delta_+(f^n \to f^{n+1}) = E_{\text{metal}}[4f^{n+1}(5d6s)^{m-1}]$$
$$- E_{\text{metal}}[4f^n(5d6s)^m].\qquad(2)$$

Charge neutrality of the final-state cell is again

imposed by demanding the presence of $m - 1$ $5d$-$6s$ electrons in the final state of Eq. (2).

Atomic solutions form an essential component of our method, and Sec. II is concerned with free-atom information. We first present estimates of $4f$ binding energies for the free-atom ground states obtained using one-electron energies and atom −ion total energy differences. The results are of interest in themselves because the ground-state free atoms generally have one more $4f$ electron than a cell in the metal. We go on to report $4f$ binding energies for the $4f^n5d^{m-1}6s$ atomic states; these configurations serve as inputs to our band calculations for the initial state metallic cells since they most closely correspond to the ground-state electron distributions of the solids. Experimental binding energies derived from atomic and ionic spectral information are also given; for a few of the ground states recent photoemission determinations have been made.

Section III deals with results for the metals. The primary intent of assembling RHF and experimental binding energies in Sec. II is to glean estimates of correlation energy contributions to $\Delta_\pm$, and this is done in Sec. III A. Band positions and $\Delta_\pm$ are discussed in Sec. III B, with particular emphasis on Δ_+. The sum

$$U = \Delta_-(f^n \to f^{n-1}) + \Delta_+(f^n \to f^{n+1})\qquad(3)$$

is the energy separation between the occupied and unoccupied $4f$ levels, and it may also be interpreted as the Coulomb interaction energy between two $4f$ electrons at the same metallic site. In Sec. III C we find $U \sim 5$–7 eV across the lanthanide row, in consonance with photoemission information. A simple estimate of cohesive energies is described in Sec. IV. In the Appendix we examine the rela-

tion between the quantities we calculate and those of the Anderson model as applied to mixed-valence systems.

II. FREE-ATOM 4f BINDING ENERGIES

A. Atomic ground states

With the exception of La, Ce, Gd, and Lu, the free rare-earth atoms have the $4f^n6s^2$ electron configuration. The ground levels determined from spectroscopic data[3] are listed in Table I; aside[4] from Ce, the states are those specified by Hund's rules. Figure 1 displays the 4f binding energies determined from our RHF calculations for these configurations. The lowermost line of the figure represents the binding energies calculated from the difference between the free-atom total energy $E(f^n$ atom) and the total energy $E(f^{n-1}$ ion) of the ion having $n-1$ 4f electrons. The RHF solutions are generated by means of the average of LS configuration scheme[5] which involves averaging over the L, S, M_L, and M_S quantum numbers of the open shells (averaging is necessary to reduce the RHF problem to the manageable solution of a set of coupled radial equations). A complete self-consistent RHF calculation is performed for both atom and ion. We have adjusted $E(f^n$ atom) and $E(f^{n-1}$ ion) to correspond to the Hund's rule states through the application of multiplet theory; the procedure is described in the appendix to I. From the $4f^n$ initial state several $4f^{n-1}$ multiplet levels may be reached by photoejection of a 4f electron; in general, the Hund's rule state is lowest, and so the bottom line of Fig. 1 represents the minimum RHF 4f excitation energy.

The upper two lines of Fig. 1 show the magnitude

TABLE I. Ground levels of the neutral lanthanide atoms (from Ref. 3).

Element	Ground level
La	$5d6s^2\ {}^2D_{3/2}$
Ce	$4f5d6s\ {}^1G_4$
Pr	$4f^36s^2\ {}^4I_{9/2}$
Nd	$4f^46s^2\ {}^5I_4$
Pm	$4f^56s^2\ {}^6H_{5/2}$
Sm	$4f^66s^2\ {}^7F_0$
Eu	$4f^76s^2\ {}^8S_{7/2}$
Gd	$4f^75d6s^2\ {}^9D_2$
Tb	$4f^96s^2\ {}^6H_{15/2}$
Dy	$4f^{10}6s^2\ {}^5I_8$
Ho	$4f^{11}6s^2\ {}^4I_{15/2}$
Er	$4f^{12}6s^2\ {}^3H_6$
Tm	$4f^{13}6s^2\ {}^2F_{7/2}$
Yb	$4f^{14}6s^2\ {}^1S_0$
Lu	$4f^{14}5d6s^2\ {}^2D_{3/2}$
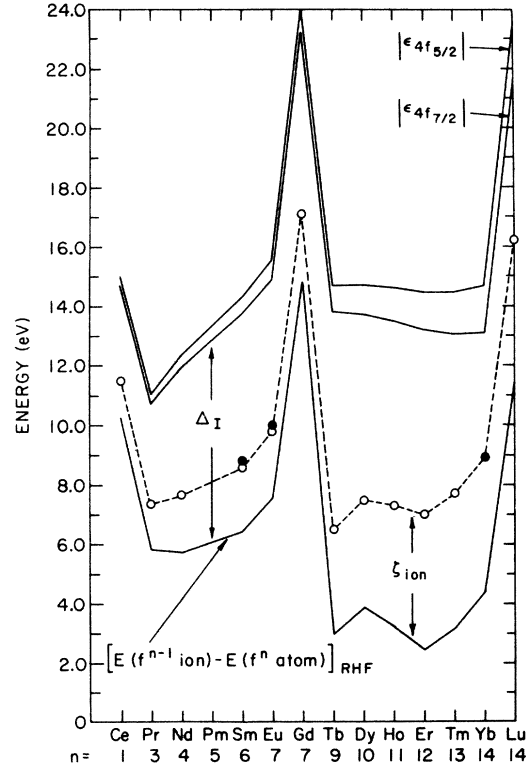
FIG. 1. 4f-electron binding energies for the ground states of rare-earth atoms. The upper two lines connect the calculated 4f one-electron energies, while the lowest line represents the 4f binding energies computed from atom → ion total energy differences. The open circles are experimental estimates of the 4f binding energies. In particular, they represent the sum of the free-atom ionization energy plus the energy difference between the ion ground state and the ion state having one fewer 4f electron (but the same charge). The filled circles for Sm, Eu, and Yb represent 4f binding energies measured directly by photoemission from metal vapors. Δ_I is the calculated intra-atomic screening energy [see Eq. (4)], and ζ_{ion} is the correlation energy difference for these transitions [i.e., the difference between the experimental and RHF 4f binding energies; see Eq. (8)]. n is the number of 4f electrons in the initial state.

of the $4f_{5/2}$ and $4f_{7/2}$ one-electron eigenvalues of the initial state; the difference between them is the 4f spin-orbit splitting, which increases monotonically across the row as is to be expected. The ϵ_{4f} emerging from the RHF computations have been modified to correspond to the Hund's rule ground state for a given f^n configuration by the addition of

$$(2/n)\delta E(4f-4f) + (1/n)\delta E(4f-5d),$$

where $\delta E(4f\text{-}4f)$ is the correction to $E(f^n$ atom) necessary for placing the 4f electrons into the appropriate ground state, and $\delta E(4f\text{-}5d)$ is the analo-

gous correction for the 4f-5d interaction; there is no 4f-6s term since the 6s shell is closed.

An estimate of the intra-atomic screening energy $\Delta_I(4f)$ associated with the relaxation of the atomic wave functions after photoionization of a 4f electron is also provided by Fig. 1,

$$\Delta_I(4f) = |\epsilon_{4f}| - [E(f^{n-1} \text{ ion}) - E(f^n \text{ atom})]; \quad (4)$$

this is simply the difference between the one-electron and total energy difference results for the 4f binding energy. If the Koopmans theorem were valid there would be no relaxation of the remaining electrons in the presence of the 4f hole, $|\epsilon_{4f}|$ would define the 4f binding energy, and $\Delta_I(4f)$ would be zero. We see from the figure that $\Delta_I(4f)$ ranges from 4 to 11 eV and is thus of the same order as the 4f excitation energy.

Lee and co-workers have recently conducted photoemission experiments[6] on Sm, Eu, and Yb vapors. Their values for the minimum 4f binding energy, corresponding to the Hund's rule ionic final state, are given by the filled circles of Fig. 1. Similar experimental information for these as well as the other lanthanide atoms may be derived by combining the ionization potentials with estimates of the ion spectral term energies.[7] For example, the ionization potential for Eu is[3] 5.7 eV and represents the energy difference between the $4f^7 6s^2(^8S_{7/2})$ free-atom ground state and the $4f^7 6s(^9S_4)$ ionic ground level. The ion spectral term estimates[7] give 4.1 eV for the separation between the $4f^7 6s(^9S_4)$ state and the $4f^6 6s^2(^7F_0)$ level, which is the lowest ionic configuration having one fewer 4f electron. Together these values imply a minimum 4f binding energy of 9.8 eV. Analogous results for the other rare-earth free atoms are given by the open circles of Fig. 1. It is clear that the direct photoemission result and the alternative estimate are in good agreement for Sm, Eu, and Yb, indicating the reliability of the methods used[7] to estimate the ion level energies.

B. $4f^n 5d^{m-1} 6s$ atomic states

Our calculations for the metals rely upon the renormalized atom method,[8] an element of which is a set of wave functions for the atomic configurations most closely approximating the electron occupation of a Wigner-Seitz cell of the solid. In contrast to the free atoms, the rare-earth metals are all trivalent, except for divalent Eu and Yb. Band-structure work and photoemission measurements indicate strong 5d character in the density of states.[9] Accordingly, we have chosen the $4f^n 5d^{m-1} 6s$ atomic configurations as starting points for initial state calculations in the metal; that is, two 5d electrons are present for the trivalent ele-
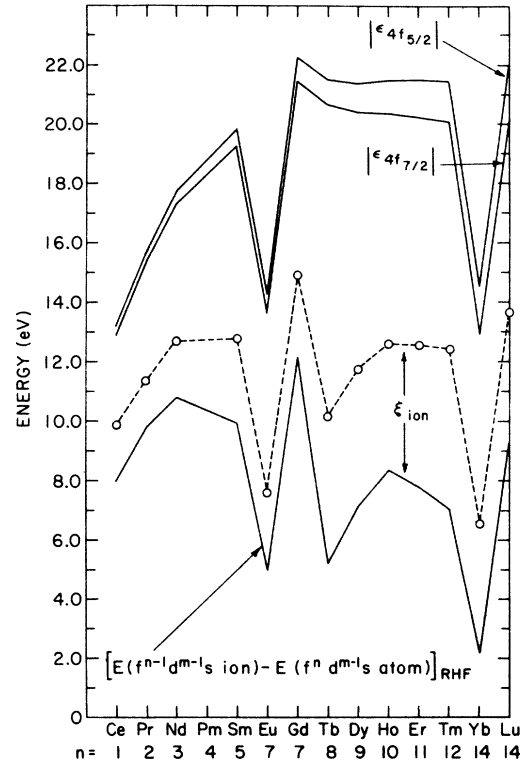
FIG. 2. 4f-electron binding energies for the $4f^n 5d^{m-1} 6s$ rare-earth free-atom configurations. The upper two lines connect the 4f one-electron energies, and the lowest line represents the 4f binding energies calculated from atom → ion total energy difference. The open circles are experimental values derived from spectral information; they result from combination of three terms; the free-atom ionization energy, the energy difference between the free-atom ground state and the $4f^n 5d^{m-1} 6s$ state, and the energy difference between the free-ion ground state and the $4f^{n-1} 5d^{m-1} 6s$ ion state. ξ_{ion} is the correlation energy difference for these transitions [see Eq. (9)], and n is the number of 4f electrons in the initial state.

ments and one for Eu and Yb.

Figure 2 displays the 4f binding energies given by both the one-electron eigenvalues and atom → ion total energy differences. As in the preceding subsection, all initial and final states have been made to correspond to the Hund's rule levels through application of multiplet theory. The 4f spin-orbit splittings of Figs. 1 and 2 are the same to within 0.05 eV, even though the 4f occupation numbers of a given element are different in many instances. For Ce, Eu, Gd, Yb, and Lu, whose valence is the same in both figures, the 4f binding energy obtained from the total energy difference is lower in Fig. 2 than in Fig. 1 because the spatially more compact 5d electron substituted for a 6s electron serves to screen the nucleus more effec-

tively, consequently reducing the binding energy. The $4f$ occupancy n is decreased by one in going from Fig. 1 to Fig. 2 for the other elements; in these cases the shielding of the nucleus by the highly localized $4f$ shell is decreased, and the $4f$ binding energy increases in going to Fig. 2.

Experimental estimates of the $4f$ binding energies for these configurations may be derived by coupling free-atom and free ion spectral information with the measured ionization potentials. We take neodymium as an example to illustrate the procedure. The Nd ionization potential is the $f^4s^2 \rightarrow f^4s$ ground-state energy difference, and spectral information[7,10] furnishes the atomic $f^4s^2 \rightarrow f^3d^2s$ and ionic $f^4s \rightarrow f^2d^2s$ splittings. Combination of the three values yields the $f^3d^2s \rightarrow f^2d^2s$ ground-state energy difference, which is the minimum $4f$ binding energy for the f^3d^2s atomic configuration of interest here. Results obtained in this way for all the lanthanide atoms are given by the open circles of Fig. 2. It is to be emphasized, however, that the spectral data are uncertain for many of the states. Since Figs. 1 and 2 present both experimental and RHF binding energies, correlation energy differences may be readily extracted from them, but we defer discussion of these until Sec. III.

III. RESULTS FOR THE METALS

In I we described in detail our method for calculating the occupied $4f$ level positions $\Delta_-(f^n \rightarrow f^{n-1})$. Within the approximations of our approach Eq. (1) for Δ_- can be reduced to

$$\Delta_-(f^n \rightarrow f^{n-1}) = \xi(f^n \rightarrow f^{n-1}) + E_{\text{metal}}^{\text{RHF}}[4f^{n-1}(5d6s)^{m+1}]$$
$$- E_{\text{metal}}^{\text{RHF}}[4f^n(5d6s)^m], \qquad (5)$$

where ξ is the free atom correlation energy correction discussed in Sec. II B of I and $E_{\text{metal}}^{\text{RHF}}$ is the total RHF energy of all the electrons in a Wigner-Seitz cell of the solid. For the unoccupied $4f$ levels $\Delta_+(f^n \rightarrow f^{n+1})$ the same initial state calculations are utilized, but the final state has one more $4f$ and one fewer $5d$-$6s$ conduction electron in keeping with the assumption of charge neutrality

$$\Delta_+(f^n \rightarrow f^{n+1}) = \xi_+(f^n \rightarrow f^{n+1}) + E_{\text{metal}}^{\text{RHF}}[4f^{n+1}(5d6s)^{m-1}]$$
$$- E_{\text{metal}}^{\text{RHF}}[4f^n(5d6s)^m]; \qquad (6)$$

ξ_+ is the analogous free-atom correlation contribution. In essence, we have replaced the problem of a single $4f^{n-1}$ or $4f^{n+1}$ impurity in a $4f^n$ host by the question of finding the energy per cell required to alter the valence of the entire metal; the latter is a far more tractable problem. Equations (5) and (6) both embody the additional assumption that correlation effects related to $4f$ excitation in the

metals are well approximated by those in the free atoms; this is a quite plausible ansatz for the highly localized $4f$ states.

A. Correlation energy contribution

For the trivalent metals the free-atom transition corresponding to $\Delta_+(f^n \rightarrow f^{n+1})$ is $4f^n 5d^2 6s \rightarrow 4f^{n+1} 5d6s$, and the associated correlation energy difference is

$$\xi_+(f^n \rightarrow f^{n+1}) \equiv E_{\text{corr}}(f^{n+1}ds) - E_{\text{corr}}(f^n d^2 s)$$
$$= [E(f^{n+1}ds) - E(f^n d^2 s)]_{\text{expt}}$$
$$- [E(f^{n+1}ds) - E(f^n d^2 s)]_{\text{RHF}}. \qquad (7)$$

The spectral data[10] provide the term in the first set of square brackets in Eq. (7), while the term in the second set of square brackets is derived from our RHF calculations for the same transition. Both initial and final configurations entering Eq. (7) for ξ_+ are electrically neutral states; the difference between them is the replacement of a $4f$ by a $5d$ electron. From the preceding subsection we may obtain correlation energy differences for atom $\rightarrow$ ion transitions in which a $4f$ electron is removed from the initial state, leaving a final state ion with unit positive charge.

The separation between the lowest two lines of Fig. 1 is the correlation energy difference ζ_{ion} for which the initial state is the ground free-atom configuration

$$\zeta_{\text{ion}}(f^n \rightarrow f^{n-1}) \equiv E_{\text{corr}}(f^{n-1} \text{ ion}) - E_{\text{corr}}(f^n \text{ atom})$$
$$= [E(f^{n-1} \text{ ion}) - E(f^n \text{ atom})]_{\text{expt}}$$
$$- [E(f^{n-1} \text{ ion}) - E(f^n \text{ atom})]_{\text{RHF}}. \qquad (8)$$

Similarly, Fig. 2 yields correlation energy differences ξ_{ion} for the $4f^n 5d^{m-1} 6s$ (atom) $\rightarrow 4f^{n-1} 5d^{m-1} 6s$ (ion) transition (i.e., the initial state is that atomic one we view as appropriate to the metal),

$$\xi_{\text{ion}}(f^n \rightarrow f^{n-1}) \equiv E_{\text{corr}}(f^{n-1} d^{m-1} s) - E_{\text{corr}}(f^n d^{m-1} s)$$
$$= [E(f^{n-1} d^{m-1} s) - E(f^n d^{m-1} s)]_{\text{expt}}$$
$$- [E(f^{n-1} d^{m-1} s) - E(f^n d^{m-1} s)]_{\text{RHF}}. \qquad (9)$$

Figure 3 displays ζ_{ion}, ξ_{ion}, and $\xi_+(f^{n+1} \rightarrow f^n)$; the last quantity is equal to $-\xi_+(f^n \rightarrow f^{n+1})$, and it has been plotted because it corresponds to transitions having one fewer $4f$ electron in the final state, as do ζ_{ion} and ξ_{ion}. The ξ_+ values for Eu and Yb are for the $f^7 ds \rightarrow f^6 d^2 s$ and $f^{14}ds \rightarrow f^{13}d^2 s$ transitions, respectively; that is, they involve trivalent initial states.

We observe that all three quantities have positive values for each of the elements. Since the RHF calculations are variational, $E_{\text{corr}} = E_{\text{expt}} - E_{\text{RHF}}$ is always a nonpositive number; hence, the positive
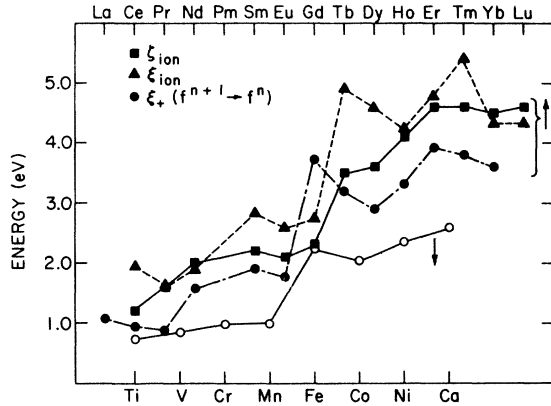
FIG. 3. Free-atom correlation energy differences. ζ_{ion}, ξ_{ion}, and $\xi_+(f^{n+1} \to f^n)$ are defined by Eqs. (7)–(9) and pertain to the rare earths. The open circles represent the correlation energy differences for the transition between ground multiplets of the divalent $3d^{n+1}$ and trivalent $3d^n$ configurations of the iron series elements. Note the general tendency of the correlation energy difference to increase across the series.

values of ζ_{ion}, ξ_{ion}, and ξ_+ imply that E_{corr} is of greater magnitude for the state with one more $4f$ electron, as we can see from the definitions given by Eqs. (7)–(9). This result conforms to the intuitive expectation that correlation effects should become more significant as the number of $4f$ electrons increases. In our nonrelativistic work[2] the analog of ξ_+ was negative. Fortunately, the inclusion of relativistic effects has produced the intuitively expected sign.

The three curves show a jump where the $4f$ shell becomes over half-filled, that is, at the point where the removed $4f$ electron is of minority spin. This occurs at Tb for ζ_{ion} and ξ_{ion} and at Gd for ξ_+ since the transition is $f^8 \to f^7$ in each case. The minority spin electron has no exchange coupling to the spherically symmetric majority spin shell and experiences strong correlation with it. A similar effect prevails for d states. The open circles of Fig. 3 represent the correlation energy difference for the $d^{n+1}(2+\text{ion}) \to d^n(3+\text{ion})$ transition in the $3d$ series[11]; the sharp rise at the middle of the row is clear.

Figure 3 shows that ξ_+ is always smaller than ζ_{ion} and ξ_{ion} for transitions involving the same numbers of $4f$ electrons. The reason for this is that some correlation energy is associated with the $5d$ electron which replaces a $4f$ in the transitions defining ξ_+, whereas a $4f$ electron is simply removed in the other cases. The disparity is larger in the second half of the series because the $4f$ correlation effects are stronger there.

The free-atom transition appropriate to Δ_- for the trivalent metals is $f^n d^2 s \to f^{n-1} d^3 s$, but no atom-

ic spectral information is available for estimating correlation energy contributions. In Refs. 1 and 2 we approximated $\xi(f^n \to f^{n-1})$ by $\xi_+(f^{n-1} \to f^n)$, which involves the same f electron numbers but corresponds to the preceding element in the Periodic Table. We can crudely assess the severity of this approximation by comparing ζ_{ion} and ξ_{ion} for neighboring elements in Fig. 3. For example, $\zeta_{ion}(\text{Dy})$ and $\xi_{ion}(\text{Ho})$ both pertain to $f^{10} \to f^9$ and differ by 0.6 eV, while the disparity is 1.1 eV between $\zeta_{ion}(\text{Tb})$ and $\xi_{ion}(\text{Dy})$, each of which is defined by an $f^9 \to f^8$ transition. Given the uncertainties in the spectral data and the dubious procedure of extrapolating the ion results to the neutral final states, however, we can only surmise that the ξ values entering Δ_- may be uncertain by as much as ~1 eV. Of course, this is in addition to the inexactitude of our assumption that correlation effects associated with the processes of interest here are identical in the metals and atoms.

B. Band positions and 4f excitation energies $\Delta_\pm$

As described in I, our band calculations for both the initial and final states of $\Delta_\pm$ are iterated to crude self-consistency through the imposition of a 0.005 eV convergence criterion on the $5d$-band extrema $\epsilon_{d\,max}$, $\epsilon_{d\,min}$ and the conduction-band minimum ϵ_{Γ_1}. The Fermi level ϵ_F is determined by assuming a parabolic s-band and a rectangular d-band density of states. To be sure, this is a great oversimplification, but it suffices for our purposes since we ultimately desire *differences* in total energies per cell and also because the bands are almost empty. $5d$-$6s$ hybridization is not included.
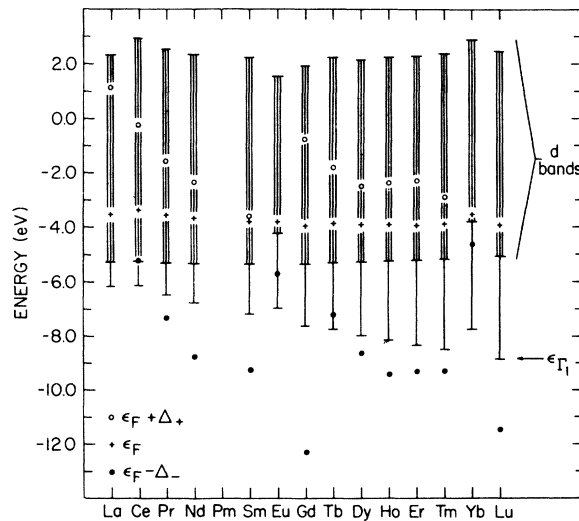
FIG. 4. Band positions, Fermi levels, and $\Delta_\pm$ estimates for the rare-earth metals.

Figure 4 shows the extent of the d bands, given by $\epsilon_{d_{max}}$ and $\epsilon_{d_{min}}$, the Fermi level, and ϵ_{r_1} obtained from our initial state calculations for each of the metals (we have neglected promethium, which is radioactive). The d bands are 7–8 eV wide for the trivalent metals. Divalent Eu and Yb have $4f$ complements larger by one than trivalency would dictate; the increased nuclear screening is responsible for larger lattice constants, leading in turn to narrower (5–7 eV) d bands. ϵ_{r_1} progressively decreases across the row while the d bands occupy roughly the same energy region.

Δ_- values corresponding to Hund's rule final (as well as initial) states are plotted as effective single-particle results in Fig. 4; in I these quantities

were treated in depth and compared with experiment. Here we focus attention on our relativistic calculations of Δ_+, which have not been reported previously.

Calculation of an unoccupied $4f$ level position in our scheme presumes a final state having one more $4f$ and one fewer conduction electron than the initial state to insure charge neutrality. There are in general many multiplet levels of the $4f^{n+1}$ configuration, and we concentrate on the excitation energy for the final state having the Hund's rule $4f^{n+1}$ ground multiplet. Δ_+ is thus an estimate of the energy of the lowest unoccupied $4f$ level. Equation (6) for Δ_+ decomposes into four conceptually simple components

$$\Delta_+ = \xi_+ + [E(f^{n+1}ds) - E(f^n d^2 s)]^{RHF}_{(LS\,av)} + [E(f^{n+1}) - E(f^n)]_{HRC} + \{ [E^{RHF}_{band}(f^{n+1}(ds)^2) - E^{RHF}_{(LS\,av)}(f^{n+1}ds)]$$

$$- [E^{RHF}_{band}(f^n(ds)^3) - E^{RHF}_{(LS\,av)}(f^n d^2 s)]\}$$

$$\equiv \xi_+ + \delta E(\text{atom}) + \delta E(\text{Hund}) + \delta E(\text{atom} \to \text{metal}) , \tag{10}$$

where HRC is the $4f$ Hund's rule correction.

We have written Eq. (10) specifically for the trivalent elements (three $5d$-$6s$ conduction electrons in the initial state, two in the final state) since we have not calculated Δ_+ for Eu due to the lack of spectral data necessary to find ξ_+. $\delta E(\text{atom})$ is the difference between the initial- and final-state total energies from our average of LS-configuration atomic calculations; $\delta E(\text{Hund})$ is the correction required to place the $4f$ electrons in the proper initial- and final-state Hund's rule multiplets (the procedure is described in the Appendix of I); and $\delta E(\text{atom} \to \text{metal})$ is the free atom $\to$ metal difference in excitation energy obtained through our self-consistent band calculations for the $5d$ and $6s$ electrons. These components of Δ_+ are listed in Table

II; Δ_+ is also represented by the open circles of Fig. 4. From Table II, it can be seen that the sum $\xi_+ + \delta E(\text{atom} \to \text{metal})$ varies over a somewhat smaller range than does $\delta E(\text{atom}) + \delta E(\text{Hund})$, which is the sum of the atomic RHF terms alone. The trend in the latter combination is qualitatively similar to that of Δ_+, but the correlation (ξ_+) and band effects $[\delta E(\text{atom} \to \text{metal})]$ produce quantitative differences. As indicated in Sec. III A, the negative sign of ξ_+ implies greater correlation in the $4f^{n+1}$ state; the positive values of $\delta E(\text{atom} \to \text{metal})$ simply mean that the energy lowering due to band effects is greater for the state with more conduction electrons, the initial state in this case. In the analogous decomposition of Δ_- made in I $\delta E(\text{atom} \to \text{metal})$ is negative because the final state

TABLE II. Components of Δ_+ (both initial and final $4f$ states are Hund's rule ground levels). See Eqs. (7) and (10) for definition of these terms; all energies in eV.

Element	ξ_+	$\delta E(\text{atom})$	$\delta E(\text{Hund})$	$\delta E(\text{atom} \to \text{metal})$	Δ_+
La	−1.1	3.3	−0.1	2.5	4.7
Ce	−0.9	2.6	−1.1	2.5	3.1
Pr	−0.9	2.0	−1.7	2.6	2.0
Nd	−1.6	1.5	−1.1	2.5	1.3
Sm	−1.9	0.7	−1.2	2.6	0.2
Gd	−3.7	0.2	4.1	2.6	3.2
Tb	−3.2	0.0	2.6	2.7	2.1
Dy	−2.9	−0.1	1.7	2.7	1.4
Ho	−3.3	−0.2	2.3	2.8	1.6
Er	−3.9	−0.2	2.9	2.8	1.6
Tm	−3.8	−0.2	2.1	2.9	1.0

has more occupied conduction states.

Unfortunately, there is little experimental information regarding the unoccupied 4f states. A few x-ray emission and appearance potential spectroscopy investigations have been conducted for some of the lighter rare-earth metals, lanthanum and cerium in particular, but the interpretation of the observed structures is still not definite. A very promising technique for probing the electronic structure of ferromagnetic materials is magneto-optical Kerr effect spectroscopy.[12,13] Measurements[12] for gadolinium indicate an unoccupied 4f level 4.6 eV above ϵ_F, which is to be compared with our result of 3.2 eV (see Table II and Fig. 4). One possibility for the discrepancy is that the final state of our Δ_+ calculation does not accurately describe the experimental situation for magneto-optical absorption. In regard to the occupied 4f level in Gd, Erskine and Flynn[13,14] have suggested that the disparity of about 2 eV between the 4f thresholds observed by optical absorption, magneto-optical absorption, and x-ray absorption on the one hand and x-ray photoemission on the other may stem from different screening configurations in the final states. Our Δ_- results are in accord with the photoemission determinations.[1,2]

We observe from Fig. 4 that Δ_- is small for Ce, Eu, and Yb, and Δ_+ is small for Sm and Tm. The minimal values imply that valence instabilities involving 4f-conduction-electron conversion will be most probable for these elements. Such instabilities can be generated by temperature and pressure changes, for instance, or by compound formation. Mixed-valence compounds such as $CeSn_3$, SmB_6, EuTe, TmSe, and $YbAl_2$ provide the most striking examples of fluctuating valence behavior.

C. Coulomb energy U

Values of $U = \Delta_+ + \Delta_-$, the energy difference between the occupied and unoccupied 4f levels, are given by the open circles of Fig. 5. The results do not differ by more than 0.5 eV from our previous, nonrelativistic estimates.[2] U varies in the 5–7 eV range, except for the 12 eV value for Gd which reflects the particular stability of its half-filled spherically symmetric 4f shell. In the simple unscreened single-particle picture U is approximated by the $F^0(4f, 4f)$ Slater integral, and our RHF calculations show this quantity to increase from 24 to 36 eV across the row (some 20% larger than the nonrelativistic F^0). The screening and relaxation effects included in the multielectron results of Fig. 5 thus reduce the single-particle estimate by a factor of roughly 5, similar to the fourfold decrease found in our nonrelativistic work.[2]
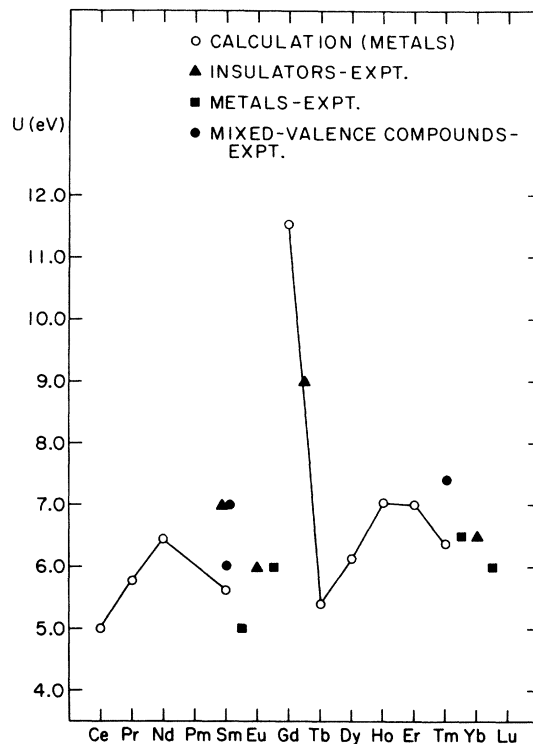
FIG. 5. Theoretical and experimental estimates of U for the rare earths. The upper and lower filled circles for Sm are obtained from XPS measurements on SmB_6 (Ref. 17) and SmS (Ref. 18), respectively. The filled circle for Tm represents an XPS determination for the Tm monochalcogenides (Ref. 19).

Hüfner and Wertheim have examined[15] x-ray-photoemission-spectroscopy (XPS) data for metals and insulators to extract experimental estimates of U, and these are represented by the triangles and squares of Fig. 5. Most of the points are plotted midway between two elements because the estimates were obtained by considering 4f level positions in neighboring metals or from data for compounds exhibiting two valence states for the rare-earth ion which correspond to U of the adjacent metallic element. As Hüfner and Wertheim remark, the agreement of the values for insulators with the calculated and experimental metal values is a significant result, suggesting that measurements on either insulating or metallic samples yield similar estimates of U for the 4f electrons. At first, this may appear surprising since it might be expected that the different screening properties of the insulators and metals would lead to disparate U values. If U is considered as the energy separation of two 4f configurations, however, then the result is more comprehensible. So long as the screening and relaxation effects are the same for the two states, a plausible first approximation in view of the lo-

calized, atomic nature of the $4f$ wave functions, then their energy difference will be roughly independent of environment.

Direct experimental determination of U is afforded by XPS measurements on mixed-valence compounds which exhibit temporal fluctuations between two configurations whose $4f$ occupation numbers differ by unity.[16] Photoexcitation evidently occurs on a time scale longer than that of the fluctuations because two sets of $4f$ structures are observed in the spectra, and they correspond to two distinct initial states; hence, the XPS measurement reveals the energy difference U between the two configurations. Values measured[17-19] for Sm and Tm compounds are given by the filled circles of Fig. 5 and are in agreement with our calculations for the metals.

IV. COHESIVE ENERGY

The energy required to form separated neutral atoms from the solid at absolute zero is the cohesive energy E_c. Our calculations for the free-atom ground states and the metals may be combined to furnish a rough assessment of E_c in the following manner:

$$E_c = \xi_c + [E(\text{ground atom}) - E(\text{metal})]_{\text{RHF}}$$

$$\equiv \xi_c + \delta E(\text{ground atom} \rightarrow \text{metal}). \quad (11)$$

Again we exploit the available spectral data[10] to estimate correlation effects; for the $4f^n 6s^2$ ground atomic configuration which becomes $4f^{n-1}(5d6s)^3$ on formation of the metal, for example, we use the correlation energy difference ξ_c for the associated atom → atom transition

$$\xi_c = [E(s^2) - E(d^2 s)]_{\text{expt}} - [E(s^2) - E(d^2 s)]_{\text{RHF}}. \quad (12)$$

TABLE III. Components of the cohesive energy E_c. See Eqs. (11) and (12) for definition of these terms; all energies in eV/atom.

Element	ξ_c	δE(ground atom → metal)	E_c
La	−0.6	3.7	3.1
Ce	−0.6	3.4	2.8
Pr	−1.6	3.4	1.9
Nd	−2.0	3.4	1.4
Sm	−2.4	2.5	0.1
Eu	−0.4	1.0	0.6
Gd	−0.7	2.8	2.1
Tb	−3.3	5.5	2.2
Dy	−3.0	4.5	1.5
Ho	−3.5	5.0	1.5
Er	−4.1	5.7	1.5
Tm	−4.0	4.9	0.9
Yb	−0.4	0.8	0.4
Lu	−0.7	3.3	2.6
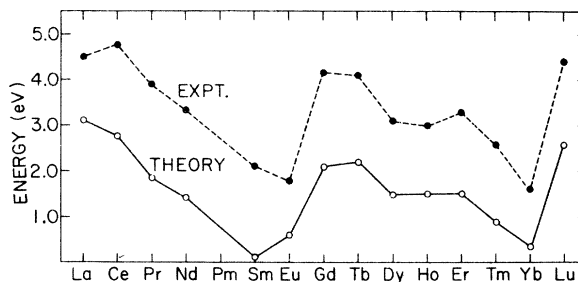
FIG. 6. Experimental values and theoretical estimates of the cohesive energies of the rare-earth metals.

The two components of E_c specified by Eqs. (11) and (12) are given in Table III. We observe that ξ_c is small for La, Ce, Eu, Gd, Yb, and Lu, each of whose $4f$ occupation number is the same for both atom and metal, while its magnitude is significantly larger for the other elements, for which the $4f$ count decreases by one on formation of the metal. In the latter cases, the sign of ξ_c points once more to greater correlation in the configuration having another $4f$ electron.

Figure 6 compares our estimates with the experimental cohesive energies furnished by Brewer and Strässler.[20] Although the shapes of the two curves are much the same, there is a discrepancy of 1.5–2.0 eV between them. Inaccurate spectral data may contribute as much as several tenths of an eV to the disparity, but we feel that the primary factor is our neglect of $5d$-$6s$ hybridization in calculating the total energy per metal cell. Inclusion of hybridization effects would have little impact on our $\Delta_\pm$ estimates since they are obtained from differences between similarly calculated total energies. This is not the case for E_c because it involves only a single total energy for the metal. Gelatt, Ehrenreich, and Watson have calculated[21] transition-metal cohesive energies via the renormalized atom method. For scandium, which has three conduction electrons, they find that the $3d$-$4s$ hybridization contributes approximately 1.8 eV to E_c; if there were an equivalent contribution for the rare-earth metals, the agreement between our crude estimates and experiment would be greatly improved.

APPENDIX: CONNECTION WITH THE ANDERSON MODEL AND INTERCONFIGURATION FLUCTUATIONS

A central feature of our $\Delta_\pm$ calculations is that each transition is confined to a Wigner–Seitz (WS) cell. Accordingly, one might expect the calculated values to be relevant to a dilute magnetic alloy, provided the radius of the WS cell used in the calculation is appropriate to that of the magnetic impurity in a particular host. [This proviso is nontrivial since the excitation of an f electron may form an ion (albeit screened) whose size is different from that of the initial ion.] This consideration is motivated by the following paradox. As mentioned in Sec. III B, there exist a number of rare-earth compounds which exhibit more than one valence; one says that the valence fluctuates or, equivalently, that there are interconfigurational fluctuations (ICF) of the 4f shells. This effect is manifested in contrasting properties, two of which we consider here. X-ray photoemission spectroscopy, a fast-time-scale measurement, yields atomiclike spectra for two 4f configurations in the ICF materials with the measured 4f binding energies, e.g., Δ_-, on the scale of eV. On the other hand, the magnetic susceptibility has a dull temperature dependence which, in general, is characteristic of *neither* 4f configuration.[22] Calculations for the Anderson model (which, of course, may be inappropriate for such concentrated systems) indicate that such a susceptibility could be explained by excitation energies on the order of 0.01 eV. Hence, the paradox: two different measurements, XPS and susceptibility, suggest Δ_- values differing by two orders of magnitude.

To explicate this paradox and provide a possible resolution we first write down the Anderson Hamiltonian

$$H_A = \sum_{\vec{k}\sigma} \epsilon_{\vec{k}} C_{\vec{k}\sigma}^\dagger C_{\vec{k}\sigma} + \sum_\sigma \epsilon_f C_{f\sigma}^\dagger C_{f\sigma} + U n_{f\uparrow} n_{f\downarrow}$$

$$+ \sum_{\vec{k}\sigma} V_{\vec{k}f} (C_{\vec{k}\sigma}^\dagger C_{f\sigma} + C_{f\sigma}^\dagger C_{\vec{k}\sigma}) . \tag{A1}$$

The first term represents the conduction band, the second and third describe a single localized nondegenerate f orbital, and the last term represents hopping between the f orbital and the conduction band. An electron may only hop from the f orbital to a conduction state having the same point symmetry as the f orbital, and so in writing H_A we implicitly restrict the $C_{\vec{k}\sigma}$ and $C_{f\sigma}$ operators to act on states of the same point symmetry. We may make the following identifications:

$$\Delta_-(f^n \to f^{n-1}) \to -\epsilon_f ,$$
$$\Delta_+(f^n \to f^{n+1}) \to \epsilon_f + U ; \tag{A2}$$

these obviously preserve the relation

$$\Delta_- + \Delta_+ = U . \tag{A3}$$

In the limit $V_{\vec{k}f} \to 0$ the Anderson parameters ϵ_f and U can be related to ground state energy differences of various 4f configurations. Within this model there is no resolution of the paradox. As Haldane points out,[23] however, H_A does not permit the local conduction-electron environment to completely adjust to a change in f occupancy, an effect which we have built into our $\Delta_\pm$ calculations. Accordingly, one can add a screening Hamiltonian to H_A of the form

$$H_{\text{scr}} = \sum_i \epsilon_i C_i^\dagger C_i + \sum_\sigma n_{f\sigma} \sum_{ij} V_{ij} C_i^\dagger C_j . \tag{A4}$$

Here the subscript i refers to conduction electrons having point symmetry *different* from that of the localized f state and V_{ij} is a Coulomb-type matrix element coupling these conduction electrons with the f states. This additional Hamiltonian accounts (at least imperfectly) for the redistribution of conduction-electron charge due to change in f occupancy. If we wished to impose charge neutrality (within a WS cell, for example) we could adjust the value of V_{ii} to do this. (In Haldane's work[23] this same idea is incorporated by imposing the Friedel sum rule.)

We consider the influence of H_{scr} on $\Delta_\pm$ in two stages; in all this we suppose $V_{\vec{k}f} = 0$. First, from the diagonal piece of the second term of H_{scr} we see that

$$\epsilon_f \to \epsilon_f + \sum_i V_{ii} \langle n_i \rangle ,$$

which, since $V_{ii} > 0$, means that the effective single-particle f level is higher in energy (that is, closer to the Fermi level) than in the absence of H_{scr}. Secondly, in the XPS experiment the transition is to a fully relaxed final state in which the conduction electrons have relaxed to the f hole. A traditional way to calculate this is to replace H_{scr} by a set of bosons (representing the particle-hole excitations in the conduction-electron gas) which are linearly coupled to n_f. In any event, one finds a positive shift energy $\Delta\epsilon$ which is equal to the square of the coupling divided by the frequency. Combining these two aspects we see that

$$\Delta_-(f^n \to f^{n-1}) = -\left(\epsilon_f + \sum_i V_{ii} \langle n_i \rangle - \Delta\epsilon \right) ,$$
$$\Delta_+(f^n \to f^{n+1}) = \epsilon_f + U + \sum_i V_{ii} \langle n_i \rangle - \Delta\epsilon ; \tag{A5}$$

we retain the relation

$$\Delta_- + \Delta_+ = U . \tag{A6}$$

On the basis of calculations for the electron gas, $\sum_i V_{ii}\langle n_i\rangle$ and $\Delta\epsilon$ are comparable. For the XPS measurement, then, Δ_- would be expected to be of order ϵ_f, i.e., a few eV. In any case Δ_- as described by Eq. (A5) contains the same physics as our calculation. But what about the susceptibility?

In the absence of any exact calculations—an extremely difficult task—we surmise that the appropriate level sampled by the susceptibility is $-(\epsilon_f+\sum_i V_{ii}\langle n_i\rangle)$, a number which could be quite small, and a small value is necessary to understand the susceptibility data on ICF compounds.

---

*Present address: Physics Dept., General Motors Research Laboratories, Warren, Michigan 48090.

[1] J. F. Herbst, R. E. Watson, and J. W. Wilkins, Phys. Rev. B 13, 1439 (1976).

[2] J. F. Herbst, D. N. Lowy, and R. E. Watson, Phys. Rev. B 6, 1913 (1972).

[3] W. C. Martin, Lucy Hagan, Joseph Reader, and Jack Sugar, J. Phys. Chem. Ref. Data 3, 775 (1974).

[4] For Ce $(4f5d6s^2)$ the Hund's rule state is $^3H_4$, while the lowest observed state is $^1G_4$; the splitting between the two is 1279 cm^{-1} = 0.16 eV [W. J. Childs and L. S. Goodman, Phys. Rev. A 1, 1290 (1970)].

[5] I. Lindgren and A. Rosén, Case Stud. At. Phys. 4, 93 (1974).

[6] S.-T. Lee, S. Süzer, E. Matthias, R. A. Rosenberg, and D. A. Shirley, J. Chem. Phys. 66, 2496 (1977).

[7] Leo Brewer, J. Opt. Soc. Am. 61, 1666 (1971).

[8] R. E. Watson, H. Ehrenreich, and L. Hodges, Phys. Rev. Lett. 24, 829 (1970); L. Hodges, R. E. Watson, and H. Ehrenreich, Phys. Rev. B 5, 3953 (1972).

[9] In this context we note that resistivity measurements on liquid Cu-R alloys (R = La, Ce, Pr, Nd, or Gd) yield an estimate of ~1.9 5d electrons per atom for each of the rare-earth components; see H.-J. Güntherodt and A. Zimmerman, Phys. Kondens. Mater. 16, 327 (1973).

[10] Leo Brewer, J. Opt. Soc. Am. 61, 1101 (1971).

[11] R. E. Watson, Phys. Rev. 118, 1036 (1960).

[12] J. L. Erskine and E. A. Stern, Phys. Rev. B 8, 1239 (1973).

[13] J. L. Erskine, Phys. Rev. Lett. 37, 157 (1976), and references therein.

[14] J. L. Erskine and C. P. Flynn, Phys. Rev. B 14, 2197 (1976).

[15] S. Hüfner and G. K. Wertheim, Phys. Rev. B 7, 5086 (1973).

[16] For a comprehensive review, see M. Campagna, G. K. Wertheim, and E. Bucher, Structure and Bonding 30, 100 (1977), and references therein.

[17] J. N. Chazalviel, M. Campagna, G. K. Wertheim, and P. H. Schmidt, Phys. Rev. B 14, 4586 (1976).

[18] M. Campagna, E. Bucher, G. K. Wertheim, and L. D. Longinotti, Phys. Rev. Lett. 33, 165 (1974).

[19] M. Campagna, E. Bucher, G. K. Wertheim, D. N. E. Buchanan, and L. D. Longinotti, Phys. Rev. Lett. 32, 885 (1974).

[20] Charles Kittel, Introduction to Solid State Physics, 4th ed. (Wiley, New York, 1971), p. 96.

[21] C. D. Gelatt, Jr., H. Ehrenreich, and R. E. Watson, Phys. Rev. B 15, 1613 (1977).

[22] See, for example, D. K. Wohlleben, and B. R. Coles, Magnetism, edited by G. T. Rado and H. Suhl (Academic, New York, 1973), Vol. V, p. 39.

[23] F. D. M. Haldane, Phys. Rev. B 15, 281 (1977); 15, 2477 (1977).